Transfer RNA(Ala) recognizes transfer-messenger RNA with specificity; a functional complex prior to entering the ribosome?

Reynald Gillet, Brice Felden

Transfer RNA^Ala recognizes transfer-messenger RNA with specificity; a functional complex prior to entering the ribosome?

Reynald Gillet and Brice Felden[1]

Laboratoire de Biochimie Pharmaceutique, Faculté de Pharmacie, Université de Rennes I, UPRES Jeune Equipe 2311, IFR 97, 2 avenue du Pr Léon Bernard, 35043 Rennes, France

[1]Corresponding author
e-mail: bfelden@univ-rennes1.fr

tmRNA (SsrA or 10Sa RNA) functions as both a transfer RNA and a messenger RNA, rescues stalled ribosomes and clears the cell of incomplete polypeptides. We report that native *Escherichia coli* tmRNA interacts specifically with native or synthetic *E.coli* tRNA alanine (tRNA^Ala) *in vitro*, alanine being the first codon of the tmRNA internal open reading frame. Aminoacylatable RNA microhelices also bind tmRNA. Complex formation was monitored by gel retardation assays combined with structural probes. Nucleotides from the acceptor stem of tRNA^Ala are essential for complex formation with tmRNA. tRNA^Ala isoacceptors recognize tmRNA with different affinities, with an important contribution from tRNA^Ala post-transcriptional modifications. The most abundant tRNA^Ala isoacceptor *in vivo* binds tmRNA with the highest affinity. A complex between tRNA^Ala and tmRNA might involve up to 140 tmRNA molecules out of 500 present per *E.coli* cell. Our data suggest that tmRNA interacts with the tRNA that decodes the resume codon prior to entering the ribosome. Biological implications of promoting specific complexes between tmRNA and aminoacylatable RNAs are discussed, with emphasis on primitive versions of the translation apparatus.
Keywords: evolution/protein synthesis/tRNA^Ala/tmRNA/*trans*-translation

Introduction

In bacteria, transfer-messenger RNA (tmRNA), known alternatively as SsrA RNA or 10Sa RNA, rescues stalled ribosomes and contributes to the degradation of incompletely synthesized peptides. As an ancillary role (Huang *et al*., 2000), this RNA encodes a peptide tag that is incorporated at the end of the aberrant polypeptide and targets it for proteolysis. This process, referred to as *trans*-translation, is frequent when *Escherichia coli* cells grow, but is not essential. The gene encoding tmRNA is, however, considered essential for *Mycoplasma genitalium* and *Mycoplasma pneumoniae* (Hutchison *et al*., 1999), and without doubt for *Neisseria gonorrhoeae* survival (Huang *et al*., 2000). Foreign and artificial mRNAs are substrates for *trans*-translation both *in vitro* and *in vivo*. In *E.coli* cells, however, the only known endogenous target for *trans*-translation is the mRNA encoding the Lac repressor

involved in cellular adaptation to lactose availability (Abo *et al*., 2000). tmRNA function is also required for the efficient growth of *Bacillus subtilis* under various stresses (Muto *et al*., 2000). Altogether, evidence suggests that tmRNA expression becomes crucial when bacteria have to adapt to environmental changes.

tmRNA acts initially as tRNA, being aminoacylated at its 3′ end with alanine by alanyl-tRNA synthetase (Komine *et al*., 1994; Ushida *et al*., 1994), to add alanine to the stalled polypeptide chain. Resumption of translation ensues not on the mRNA upon which the ribosomes were stalled, but at an internal position in tmRNA. Termination soon occurs and permits ribosome recycling. The current model is that aminoacylated tmRNA is first recruited to the ribosomal A site. Subsequently, the nascent polypeptide chain is transferred to the tRNA portion of aminoacylated tmRNA. The ribosome translocates and the incomplete mRNA is replaced with the open reading frame (ORF) of tmRNA possessing a termination codon (for a review see Karzai *et al*., 2000). Thus, tmRNA has a dual function in bacteria. First, as a tRNA, thanks to a partial structural analogy with canonical tRNAs, and then as an mRNA, with an internal coding sequence that begins, in the vast majority of known tmRNA sequences, with an alanine (resume) codon.

Primitive versions of the translation apparatus were proposed to be made solely of RNAs (Noller *et al*., 1992; Piccirilli *et al*., 1992). To study how protein synthesis may have looked some 3.8 billion years ago, before protein-based life emerged, one might contemplate designing an 'all RNA' system that can form a peptide bond. Recent structural (Nissen *et al*., 2000) and functional (Muth *et al*., 2000) evidence suggests that the ribosome is a catalytic RNA (ribozyme), and also that an aminoacyl-tRNA synthetase ribozyme can aminoacylate a tRNA (Lee *et al*., 2000). Also, iterative RNA selection previously identified ribozymes that form amide bonds between RNA and an amino acid, or between two amino acids (Zhang and Cech, 1997).

In today's cellular protein factory, the ribosome orchestrates the process of protein synthesis, bringing tRNAs and mRNAs into proximity (Figure 1A). There are intrinsic assets in selecting tmRNA as a model to form a peptide bond without the help of ribosomal proteins (Figure 1B). First, tmRNA consists of a single poly-ribonucleotide chain that sustains two main functions in protein synthesis: (i) the adapter between the genetically encoded message and the newly synthesized polypeptide (tRNA function), and (ii) the encoded message itself (mRNA function). Secondly, tmRNA occurs *in vivo* in all bacteria with a precise biological function, in contrast to *in vitro* selected RNAs. Thirdly, tmRNAs are long enough (between 260 nucleotides for the shortest sequences and ~430 nucleotides for the longer ones) to form an RNA core
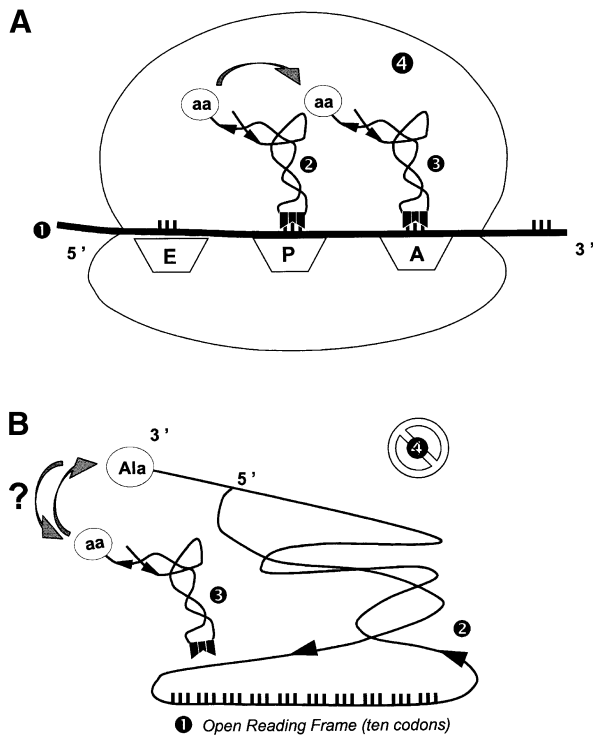
A

B

Fig. 1. Schematic illustration of (**A**) the usual 'ribosome-driven' protein synthesis compared with (**B**) an hypothetical 'tmRNA-driven' peptide bond formation. Tripartite lines are the triplets of the messenger RNA (1). RNAs that receive the amino acid during transpeptidation are either (A) a canonical tRNA or (B) tmRNA (2). A canonical tRNA (3) donates the amino acid prior to transpeptidation. The ribosome (4) is either (A) present or (B) absent. Notice that in (B), tmRNA is the mRNA and also the tRNA (1 and 2).

A

B

Fig. 2. (**A**) Native gel retardation assays between native canonical tRNAs and tmRNA from *E.coli*. Labeled native tRNA^Ala3, but not native tRNA^Asp, interacts with unlabeled tmRNA. (**B**) Labeled tRNA^Ala3 (0.5 pmol) binds tmRNA in the presence of all tRNAs from *E.coli*.

with an intricate tertiary structure, a prerequisite for an RNA that stands as a candidate for mimicking primitive versions of the translation apparatus. Fourthly, tmRNA is not a ribosomal RNA. Thus, it could have arisen before the RNA–protein-based polypeptides synthesis machinery.

As a step toward this task, we investigated whether tmRNA could interact specifically with either native or synthetic canonical tRNA(s), as well as with minimalist RNA structures for aminoacylation, as microhelices, proposed to be present when the genetic code was shaped from an operational RNA code that related RNA sequences and/or structures to specific amino acids (Schimmel *et al.*, 1993). Our initial hypothesis was that canonical tRNAs or RNA microhelices might recognize tmRNA with specificity *in vitro*. An initial recognition between tRNA and tmRNA could involve specific inter-actions outside of the tmRNA internal ORF. Subsequently, nucleotides from the anticodon of the tRNA could trigger specific pairings with matching codons of the tmRNA ORF, mimicking a 'codon–anticodon' interaction. Minimalist structures for aminoacylation might also be capable of complex formation with tmRNA. Here, we report that native *E.coli* tmRNA interacts either with native or synthetic tRNA^Ala from *E.coli in vitro*, as well as with RNA microhelices whose sequences are derived from tRNA^Ala isoacceptors. The structural basis of these specific interactions between tmRNA and aminoacylatable RNAs was defined further by chemical and enzymatic probes in
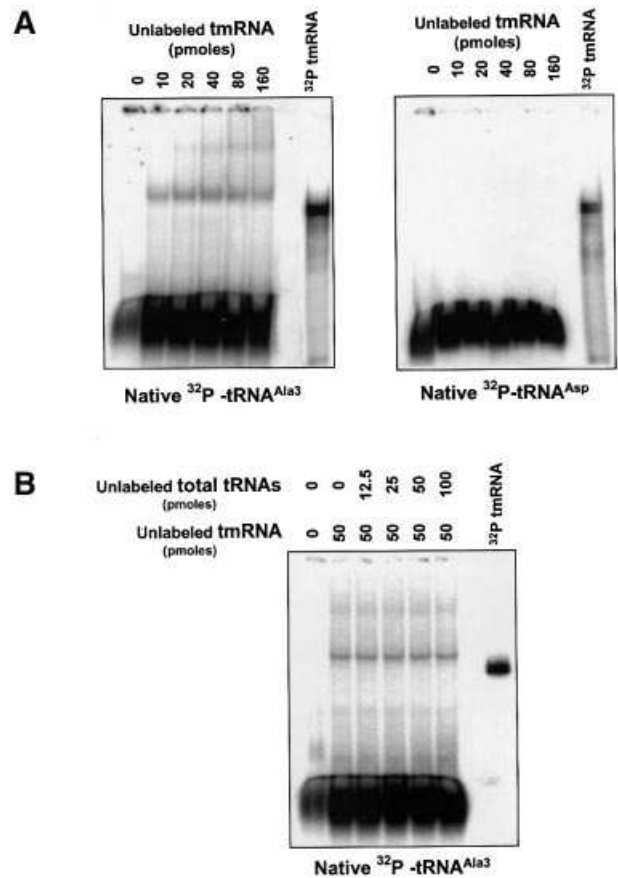
solution. Our results suggest that the tRNA that decodes the resume codon of *E.coli* tmRNA is recruited prior to its interaction with the ribosome.

Results

tRNA^Ala, but not tRNA^Asp or tRNA^Gln, binds tmRNA with specificity in vitro

Among all tRNAs, we reason that native tRNA^Ala from *E.coli* has a relatively higher advantage in binding tmRNA via a codon–anticodon interaction, since there are four alanine codons in the tmRNA ORF, including the resume codon. Monitoring the appearance of a slow-migrating band that is largely pulled apart from a 76-nucleotide labeled tRNA (size difference of 76 + 363 nucleotides) should provide an unambiguous answer as to whether or not a specific tmRNA–tRNA^Ala complex forms *in vitro*. A specific gel-retarded band is observed with labeled native *E.coli* tRNA^Ala, but not with native tRNA^Asp (Figure 2A). For tRNA^Ala, the gel-retarded band migrates slower than labeled tmRNA alone (Figure 2A, left), suggesting that the complex contains full-length tmRNA. The complex between tmRNA and tRNA^Ala involves non-covalent interactions, since the gel-retarded band disappears in the presence of 8 M urea (data not shown). With native tRNA^Asp, (one matching codon in the tmRNA ORF), there are no detectable gel-retarded bands. An ~320 molar
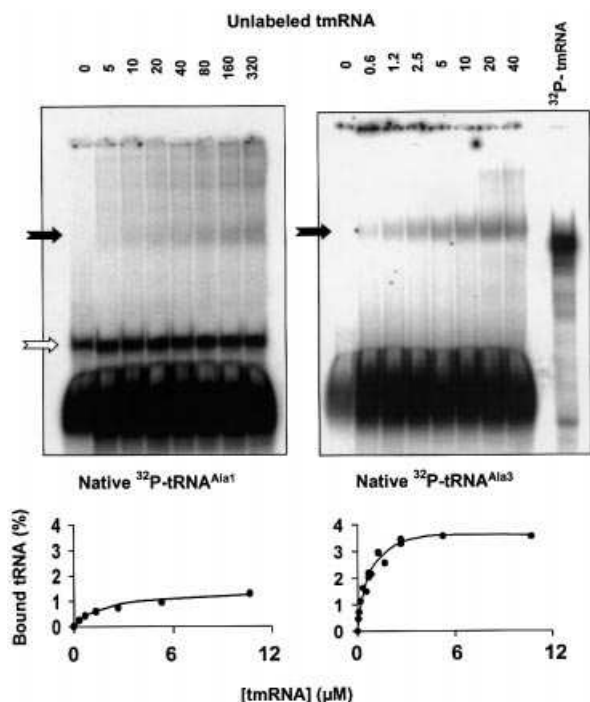
Fig. 3. Native gel retardation assays between tmRNA and native tRNA[Ala] isoacceptors 1 and 3 from *E.coli*. For native tRNA[Ala3], the binding plateaus show all the experimental values collected from four independent experiments. For native tRNA[Ala1], only the experimental values from the upper panel are shown, and six independent experiments were performed, with binding plateaus fluctuating from 1 to 2%. The black and white arrows point to tRNA[Ala]–tmRNA complexes and tRNA dimers, respectively.

Table I. Kinetic parameters of complex formation between *E.coli* tmRNA and native or synthetic aminoacylatable RNAs

RNAs	Plateau levels[a] (%)	K_d[a] (μM)
Escherichia coli tRNA[Ala] [b]		
native tRNAs		
1	1.5	3.5
3	4	0.5
in vitro transcribed tRNAs		
1	0.8	1.2
3	0.8	1.2
2	4.5	2.5
1–2	5	2.5
Escherichia coli tRNA[Ala] microhelices		
1–3	0.5	0.7
2	2	0.7
Escherichia coli tRNA[Asp]	0	n.d.
Yeast tRNA[Asp]	0	n.d.
Escherichia coli tRNA[Gln]	0	n.d.

[a]Plateau levels and K_d are $\pm$0.5% and $\pm$0.5 μM, respectively.
[b]Nomenclature and numbering of all tRNA sequences are from Sprinzl *et al*. (1998).
n.d., not determined.

excess of tmRNA is still unable to gel-shift tRNA[Asp] (Figure 2A, right), demonstrating that not all tRNAs are able to bind tmRNA. tRNA[Gln] was also assayed, since it has no matching codon within the tmRNA ORF. Upon the addition of up to a 600 molar excess of tmRNA to *in vitro* transcribed tRNA[Gln], there is no detectable complex formation (not shown). Interestingly, labeled tRNA[Ala] binds unlabeled tmRNA even in the presence of an ~200 molar excess of all tRNA isoacceptors from *E.coli* (0.5 pmol of tRNA[Ala] for 100 pmol of total tRNAs; Figure 2B).

Native E.coli tRNA[Ala] isoacceptors bind E.coli tmRNA with different affinities

In the *E.coli* tmRNA ORF, there are four alanine codons: two, including the resume codon, are 'GCA' and two are 'GCU'. Native *E.coli* tRNA[Ala] isoacceptors 1 (tRNA[Ala1]) and 3 (tRNA[Ala3]) differ in their anticodon triplet sequence, GGC and UGC, respectively, with only tRNA[Ala3] being able to form three canonical pairs with a GCA codon. Also, these two native tRNA[Ala] have identical nucleotide sequences, except at seven positions including position 34, and except for two modified nucleotides at positions 8 and 34 (Sprinzl *et al*., 1998). Gel retardation assays were performed between these two native tRNA[Ala] isoacceptors and native tmRNA from *E.coli* (Figure 3). For labeled native tRNA[Ala1] (~0.5 pmol), 10 pmol of unlabeled tmRNA are required to visualize a gel-retarded band,

which becomes darker upon increasing tmRNA concentration and migrates slower than labeled tmRNA alone (black arrow in Figure 3, left). For labeled native tRNA[Ala3], however, 0.6 pmol of unlabeled tmRNA are sufficient to observe, at a similar location to that for tRNA[Ala1], a gel-retarded band, which also becomes darker when tmRNA concentration increases (black arrow in Figure 3, right). Native tRNA[Ala1] forms dimers in solution, as indicated by an additional band (white arrow in Figure 3, left), which migrate at a slower pace than tRNA[Ala1] alone. tRNA[Ala1] from *E.coli* is known to be a 'dimer-forming' tRNA (Kholod, 1999). Native tRNA[Ala3], however, does not dimerize in solution (Figure 3, right).

For both native tRNA[Ala1] and tRNA[Ala3], the concentration of the *E.coli* tmRNA–tRNA[Ala] complex was plotted versus tmRNA concentration (Figure 3, bottom). For tRNA[Ala1], plateau levels are up to 2% with a 3.5 μM dissociation constant, whereas plateau levels of tRNA[Ala3] are up to 4% with a 0.5 μM dissociation constant (the data are from six independent experiments for each tRNA; Table I). Compared with native tRNA[Ala3], the reduced ability of native tRNA[Ala1] to bind tmRNA can be explained because of either: (i) its ability to form dimers in solution; (ii) its sequence differences at seven positions; (iii) its content in modified nucleosides differing at two positions; or (iv) the involvement of the correct anticodon to bind the resume codon, which is present in tRNA[Ala3] but not in tRNA[Ala1]. To address these issues one by one, four tRNA[Ala] constructs named tRNA[Ala1], tRNA[Ala2], tRNA[Ala3] and tRNA[Ala1–2] were designed, cloned, and their corresponding RNAs produced *in vitro* (Figure 4). Between all of the synthetic tRNA[Ala] constructs inspired by tRNA[Ala] isoacceptors, the sequence varies only at 12 positions (Figure 4, black circles), the remaining 64 nucleotides being identical. These 12 variable positions are clustered into two sets: one that gathers seven nucleotides within the acceptor branch and another that includes five nucleotides from the anticodon stem–loop.
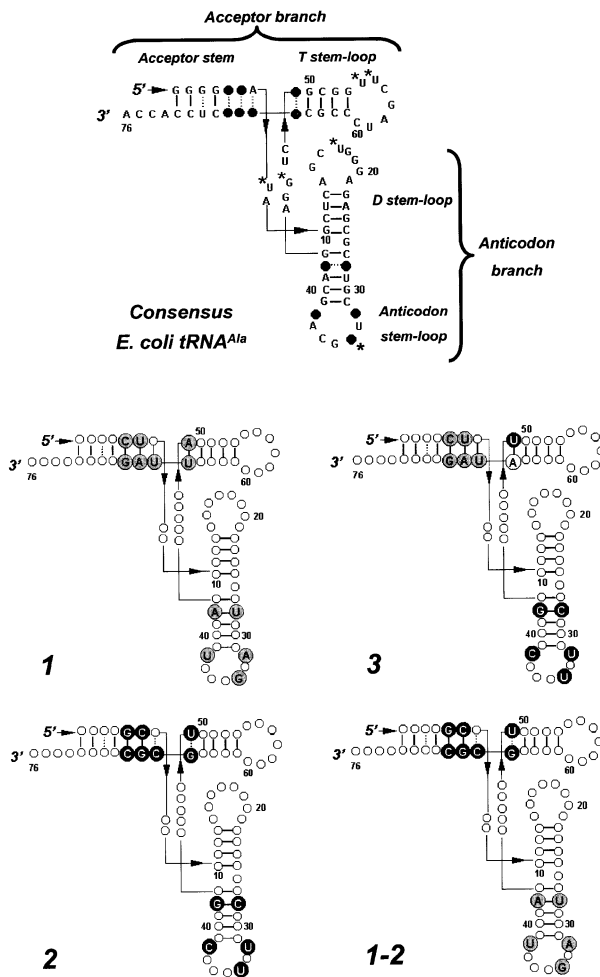
Fig. 4. Sequences and secondary structures of the purified native tRNA^Ala, as well as the synthetic tRNA^Ala constructs designed, produced and tested for binding *E.coli* tmRNA. A sequence consensus for *E.coli* tRNA^Ala secondary structure (top panel), with the black dots and stars corresponding to the location of the variable nucleotides and the post-transcriptional modifications, respectively. Native or synthetic tRNA^Ala constructs are numbered from 1 to 3 (nomenclature from Sprinzl *et al.*, 1998), with 1-2 being a chimera between 1 and 2. In all four tRNAs, invariant nucleotides are in white dots and variable nucleotides are indicated.

tRNA^Ala post-transcriptional modifications are important for binding tmRNA

Compared with their corresponding native counterparts, synthetic tRNA^Ala1 and tRNA^Ala3 bind tmRNA poorly, only up to 0.8% at the plateau (compare Figures 3 and 5). For both synthetic tRNAs^Ala deprived of modified nucleosides, a gel-retarded band that corresponds to a tRNA–tmRNA complex is only detectable when 25 pmol of unlabeled tmRNA are present (Figure 5). Nevertheless, for both RNAs the binding is specific, increases in a concentration-dependent manner and reaches a plateau that is 3- to 4-fold reduced compared with their native counterparts (Figure 5; Table I). This result demonstrates the importance of the modified bases in forming a stable complex between tmRNA and tRNA^Ala in solution.

In vitro transcribed tRNA^Ala1 also dimerizes in solution (white arrow, Figure 5), demonstrating that post-transcriptional modifications are not required for dimer formation.
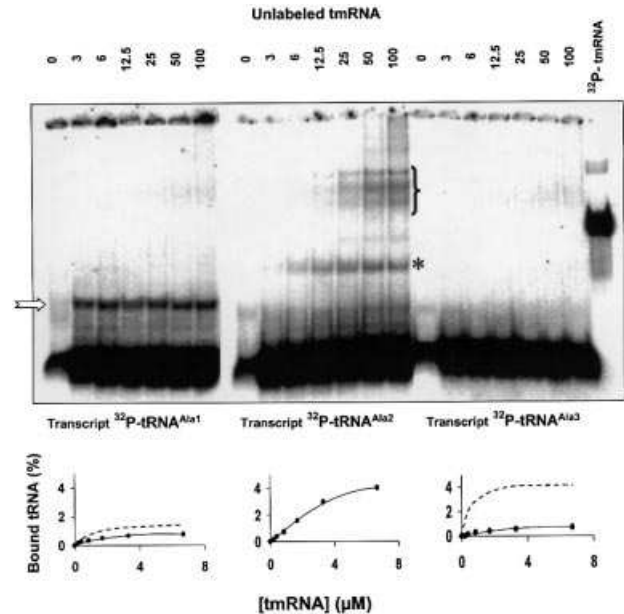

Fig. 5. Native gel retardation assays between *E.coli* tmRNA and labeled synthetic tRNA^Ala constructs 1, 2 and 3. The binding curves are derived from the experiments shown above. The experimental values were reproduced from at least three independent experiments for each synthetic tRNA. The white arrow points to tRNA dimers. For a direct comparison between natives and synthetic tRNA^Ala1 and tRNA^Ala3, the binding plateaus of their natives counterparts are indicated by dotted lines. For tRNA^Ala2, the binding curve does not include complex formation with the tmRNA fragment.

With the exception of the A_{49}-U_{65} pair, which is flipped over (U_{49}-A_{65}), tRNA^Ala3 has the acceptor branch of tRNA^Ala1 (Figure 4). Interestingly and in contrast to tRNA^Ala1, native or *in vitro* transcribed tRNA^Ala3 does not form any detectable dimers in solution. It demonstrates that minor sequence variations in the anticodon stem–loop can convert a dimer-forming tRNA to a non dimer-forming tRNA, independently of the presence or absence of modified nucleosides.

The sequence of the tRNA^Ala acceptor stem is essential for binding tmRNA

tRNA^Ala2 differs from tRNA^Ala1 at 12 positions (Figure 4). Also, this tRNA has six variable nucleotides compared with tRNA^Ala3, but an identical anticodon stem–loop (Figure 4). This tRNA alanine was originally sequenced by Williams *et al.* (1974) and has a $G_3 \cdot C^{70}$ pair instead of the $G_3 \cdot U^{70}$ pair that is required as a major determinant for aminoacylation with alanine (for a review see Varani and McClain, 2000). Thus, we purposefully changed nucleotides at positions 69 and 70 into C^{69} and U^{70} in order to design a tRNA construct that is chargeable with alanine. Considering also the *in vivo* data from two-dimensional polyacrylamide gel electrophoresis fractionation of *E.coli* tRNAs, which has characterized only two tRNA^Ala isoacceptors (Dong *et al.*, 1996), the existence of this third tRNA^Ala isoacceptor *in vivo* is highly questionable.

In vitro transcribed tRNA^Ala2 does not form any detectable dimers in solution. With tRNA^Ala2, up to 4.5% of the complex with tmRNA is formed, with a dissociation constant of 2.5 µM (Table I; Figure 5). In a concentration-dependent manner, three gel-retarded bands appear

(occasionally a smear, probably containing several conformers), together with a gel-accelerated one (asterisk, Figure 5). The bands were excised from the gel, eluted passively and reverse transcribed with a DNA oligonucleotide complementary to 13 nucleotides at the tmRNA 3′ end. Only the gel-retarded ones contain full-length tmRNA in complex with tRNA[Ala2], whereas the fast-migrating band contains a tmRNA fragment. The specific cleavage of tmRNA is a direct consequence of tRNA[Ala2] binding, since it only appears when tRNA[Ala2] is added. The tmRNA conformation is very flexible and contains several sequence stretches that are particularly unstable in solution (Felden et al., 1997).

A tRNA[Ala] chimera was also designed and produced in vitro that recapitulates the anticodon branch of tRNA[Ala1] with the accepting branch of tRNA[Ala2], and was named tRNA[Ala1–2] (Figure 4). With tRNA[Ala1–2], up to 5% of the complex with tmRNA is also formed, with a dissociation constant of 2.5 µM (Table I) and a migration pattern similar to that of tRNA[Ala2] (data not shown). tRNA[Ala2] and tRNA[Ala1–2] gel-shift tmRNA with similar (if not identical) efficiencies, both for their plateau levels and dissociation constants (Table I). This demonstrates that the nucleotide sequence at the five variable positions within the anticodon stem–loop (positions 28, 32, 34, 38 and 42) has no effect on binding, and that the sequence and/or structural elements in tRNA allowing its efficient interaction with tmRNA are elsewhere. Also, it demonstrates that sequences within tRNA[Ala2/Ala1–2] acceptor branches are responsible for a specific tmRNA fragmentation.

In vitro transcribed tRNA[Ala1] binds tmRNA very weakly, whereas tRNA[Ala1–2] is a good binder, with only seven nucleotide changes all in the acceptor branch between the two RNAs. This demonstrates that the sequence and/or structure of tRNA[Ala1–2] at these very few positions are essential for interacting with tmRNA. In vitro transcribed tRNA[Ala1] and tRNA[Ala3] have identical sequences in their acceptor branches, except for a base pair involving nucleotides 49 and 65, i.e. $A^{49} \cdot U^{65}$ in tRNA[Ala1] and $U^{49} \cdot A^{65}$ in tRNA[Ala3]. We have already demonstrated that five nucleotide differences in their anticodon branch have no effect on binding tmRNA. Since both tRNA[Ala1] and tRNA[Ala3] bind tmRNA poorly, any nucleotide combination at positions 49 and 65 that maintains pairing is of no consequence to complex formation. Out of 76 nucleotides from tRNA[Ala], the ones that are required to interact with tmRNA are within a set of five positions, all in the acceptor stem, including base pairs 5–68 and 6–67 and position 68, according to the numbering of canonical tRNAs.

Structural evidences reinforcing the implication of tRNA[Ala] acceptor stem in binding tmRNA

To characterize further the interaction, we monitored the conformation in solution of synthetic tRNA[Ala2] and native tRNA[Ala3] in the presence and absence of tmRNA, using structural probes (Figure 6). Out of the restricted set of nucleotides from synthetic tRNA[Ala2], including those required to interact with tmRNA, direct evidence for those directly involved in binding tmRNA is still missing. Also, additional structural domains other than the acceptor stem might also be involved, but not essential for complex formation. Finally, whether nucleotides from the acceptor
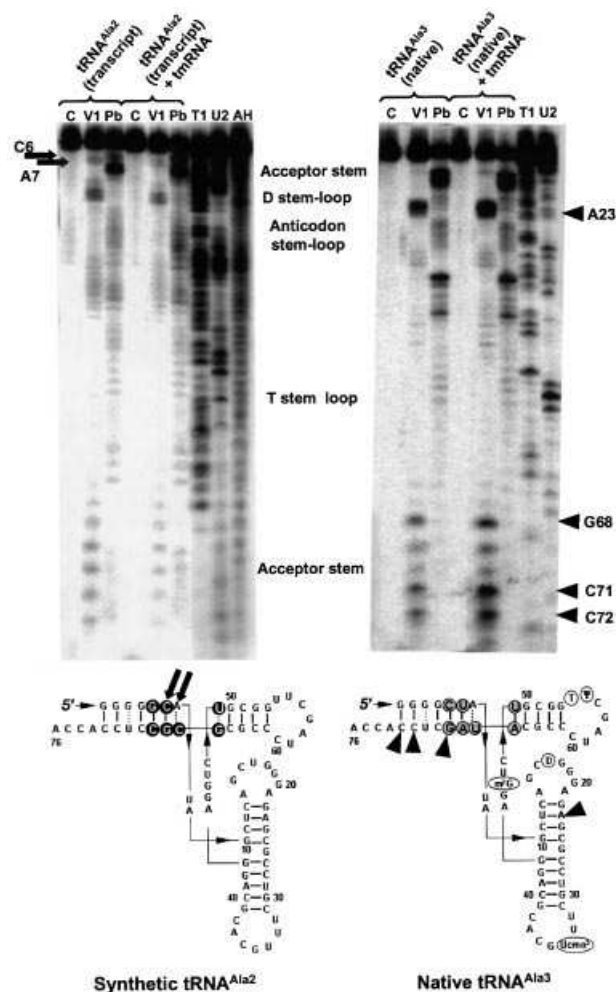

Fig. 6. Nuclease mapping and lead acetate probing data collected on native tRNA[Ala3] (right) and synthetic tRNA[Ala2] (left), in the presence or absence of tmRNA. Autoradiograms of 16% denaturing PAGE of cleavage products of 3′-labeled tRNAs, with similar migration times. Lanes C, incubation controls; lanes V1, RNase V_1 mapping; lanes Pb, lead acetate-induced hydrolysis; lanes T1, RNase T_1 hydrolysis ladder; lanes U2, RNase U_2 hydrolysis ladder; lane AH, alkaline hydrolysis ladder. For clarity, all of the five structural domains of canonical tRNAs are indicated. Mapping data differences in the presence and absence of tmRNA are indicated on tRNA[Ala] secondary structures. When tmRNA was present, only a reactivity enhancement towards structural probes was observed for specific nucleotides from both native and synthetic tRNA[Ala]. These nucleotides are marked with black arrows for lead-induced cuts and with black arrowheads for RNase V_1. For native tRNA[Ala3], the modified nucleotides are circled and nomenclature is as follows: m[7]G, 7-methylguanosine; Ucmo[5], uridine 5-oxyacetic acid; D, dihydrouridine; ψ, pseudouridine; T, ribosylthymine.

stem of native tRNA[Ala] are important for binding tmRNA remains to be established. Lead acetate cleaves RNA single strands and its specific requirements for cleavage depend on very subtle conformational changes in RNAs. Thus, it might help in deciphering discrete conformational changes in tRNA structure when in complex with tmRNA. Ribonuclease V_1, from cobra venom, cleaves RNA double strands or stacked nucleotides, and was used to monitor whether the overall architecture of synthetic or native tRNA[Ala] was altered upon binding to tmRNA. For structural probing, the experimental conditions correspond to the binding plateau derived from the gel retardation assays: 0.5 pmol of both native tRNA[Ala3] and synthetic

tRNA^{Ala2} with 20 or 50 pmol of tmRNA, respectively (Figures 3 and 5).

Except for the acceptor stem, the overall conformation of synthetic tRNA^{Ala2} is not perturbed in the absence or presence of tmRNA, as shown by identical chemical and enzymatic probing patterns (Figure 6, left). Strikingly, when tmRNA is present, the pattern of lead-induced cleavages is modified at two positions within the acceptor stem of synthetic tRNA^{Ala2}. Two nucleotides, C^6 and A^7, become reactive to lead acetate when tmRNA is present (Figure 6, left). Reactivity differences at these two positions were observed with both a 5′- and a 3′-labeled tRNA (data not shown). Of the two nucleotides, C^6 belongs to the limited set established previously as being required for complex formation with tmRNA. Also, C^6 is paired with G^{67} in the tRNA^{Ala2} secondary structure and A^7 is at the 3′ side of C^6, facing C^{68} (Figure 4). Probing data indicate that when tRNA^{Ala2} binds tmRNA, two nucleotides within the acceptor stem that are not reactive towards single-stranded specific probes in the absence of tmRNA are reactive when tmRNA is present, suggesting that the C^6-G^{67} base pair is disrupted. According to these structural probes, no differences in reactivity are observed for nucleotides 5, 67 and 68 when synthetic tRNA^{Ala2} binds tmRNA.

Strikingly, for native tRNA^{Ala3} in the presence and absence of tmRNA, the very few differences in the reactivity of nucleotides towards structural probes are also concentrated within the acceptor stem, with one exception within the D stem (Figure 6, right). An increase of RNase V$_1$-induced cuts at positions 68, 71 and 72 has been consistently observed in the presence of tmRNA. This suggests that part of the acceptor stem is stabilized further in the presence of tmRNA. Unlike synthetic tRNA^{Ala2}, positions 6 and 7 within native tRNA^{Ala3} are already cleaved by lead in the absence of tmRNA.

tRNA^{Ala} microhelices bind tmRNA

We anticipated that a minimalist RNA construct recapitulating a 7-base-pair tRNA^{Ala} acceptor stem capped by a 7-nucleotide loop might be sufficient to interact with tmRNA. For the alanine system, aminoacylation is determined by a single G^3·U^{70} pair (Francklyn and Schimmel, 1989), implying that this RNA microhelix can be aminoacylated with alanine, and, if it interacts with tmRNA, will simplify further our working system for peptide bond formation in an 'all RNA' environment.

Two RNA microhelices were designed and produced *in vitro* (Figure 7A). The sequence of microhelix 1–3 is derived from tRNA^{Ala1} and tRNA^{Ala3}. The sequence of microhelix 2 is derived from tRNA^{Ala2}, which binds tmRNA with affinity. Microhelix 1–3 forms seven base pairs, whereas microhelix 2 has only six base pairs with an A^7·C^{15} mismatch. Both microhelices bind tmRNA with specificity, demonstrating that the tRNA^{Ala} acceptor stem is necessary and sufficient to promote binding with tmRNA (Figure 7B; Table I). Also, binding of a microhelix does not require an A^7·C^{15} mismatch within the acceptor stem. Compared with full-length tRNA^{Ala}, the complex between tmRNA and RNA microhelices is gel-retarded to a lower extent, accounting for a microhelix being 3-fold smaller than a tRNA (compare the migration pattern of the gel-retarded complex in Figures 3 and 7).
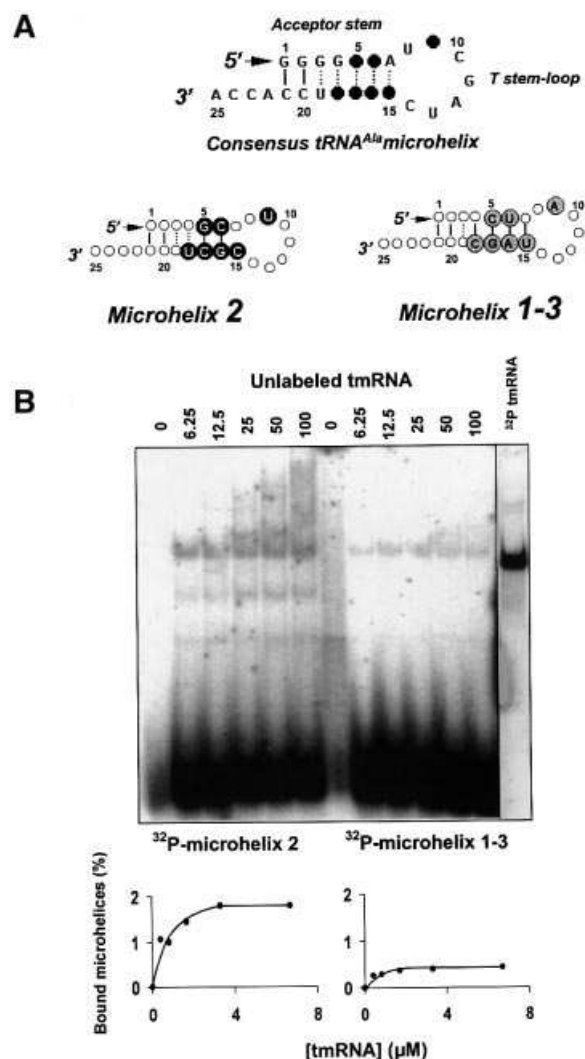

Fig. 7. Native gel retardation assays between RNA microhelices and tmRNA. (**A**) A sequence consensus (top) depicted on secondary structure models of the minimalist RNAs, with the black circles corresponding to the variable nucleotides. (**B**) The binding curves are derived from the experiment shown above. For each RNA microhelix, the experimental values were reproduced in three independent experiments.

Microhelix 1–3, as for *in vitro* transcribed tRNA^{Ala1} and tRNA^{Ala3}, binds tmRNA weakly (~0.5%), but microhelix 2, as for tRNA^{Ala2}, binds tmRNA with plateau levels 4-fold higher (2% of complex formation at the plateau; Table I). Thus, both microhelices and full-length tRNAs are recognized by tmRNA by similar rules. Also, as for tRNA^{Ala2}, there are specific cleavages of tmRNA when microhelix 2 binds tmRNA (lower bands in Figure 7B, left), but not for microhelix 1–3, as for tRNA^{Ala1} and tRNA^{Ala3}. These tmRNA fragments are still able to bind microhelix 2, as for tRNA^{Ala2}. Both microhelices bind tmRNA with similar dissociation constants (0.7 μM; Table I). For both synthetic tRNA^{Ala1} and tRNA^{Ala3}, dissociation constants are also equivalent but higher than their corresponding microhelices (1.2 μM; Table I). This suggests that these two tRNAs possess sequences and/or structural features outside of their acceptor stem that act as negative elements (anti-determinants) when binding tmRNA.
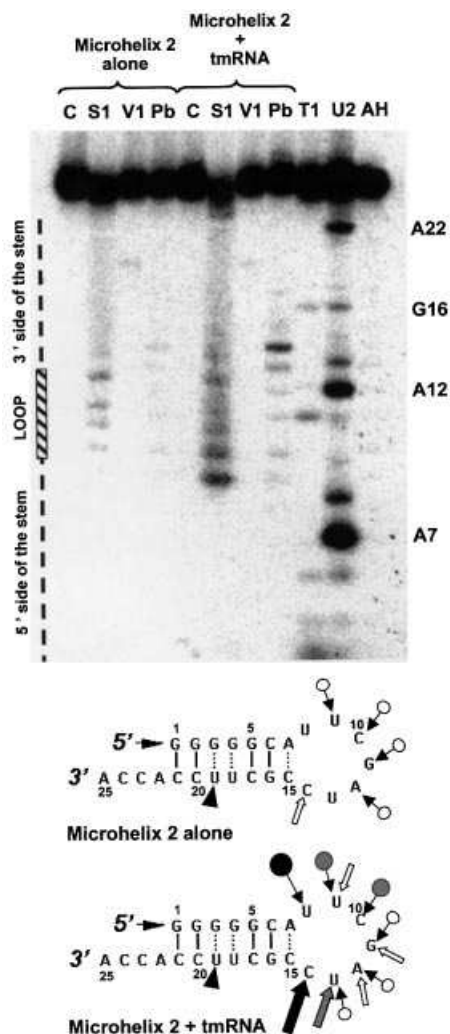
Fig. 8. Nuclease mapping and lead acetate probing data collected on RNA microhelix 2, in the presence or absence of purified tmRNA. Autoradiograms of 20% denaturing polyacrylamide gels of cleavage products of 5′-labeled RNA microhelices. Lanes S1, RNase S_1 mapping; all other lanes are as in Figure 6. Sequencing tracks are numbered every four to five nucleotides. Structural mapping data in the presence or absence of tmRNA are indicated. When tmRNA is present, only reactivity enhancement towards structural probes are observed, all located in the loop. Straight and circled arrows correspond to lead and nuclease S_1 cleavages, respectively, with the thickness and darker color referring to the intensity of cleavage (weak, medium and strong). Black arrowheads correspond to RNase V_1 cleavages. The molar ratio between microhelices and tmRNA is 100:1.

Upon binding tmRNA, the loop of the RNA microhelix unfolds

The conformations of RNA microhelices were monitored with or without tmRNA in solution, using lead acetate and RNase V_1. Nuclease S_1, specific for RNA single strands, was also used (Figure 8). The probing data will be compared with that collected with full-length tRNA[Ala] (Figure 6). In the absence of tmRNA, microhelix 2 is cut by RNase V_1 at position 19, cleaved by RNase S_1 at positions 9–12 and also by lead at position 14 (Figure 8), three arguments supporting the existence in solution of a stem capped by a loop. Strikingly, when 50 pmol of unlabeled tmRNA (corresponding to the binding plateau; Figure 7B) are added to microhelix 2, there is a significant enhancement of RNase S_1 cleavages at positions 8–10.

Also, lead-induced cleavages appear at positions 13 and 14. Positions 8–14 correspond to the seven nucleotides of the loop. RNase V_1-induced cleavage at position 19 is still visible, suggesting that the stem is still folded when RNA microhelix 2 binds tmRNA. To test whether the $A^7 \cdot C^{15}$ mismatch is what allows this large unfolding of the loop to occur, the conformation of microhelix 1–3, with or without tmRNA, was also monitored in solution. In the presence of tmRNA, a similar probing pattern was observed for microhelix 1–3, suggesting that the reactivity of its 7-nucleotide loop towards single-stranded specific probes is significantly increased when in complex with tmRNA (data not shown). All of the sequence differences between the two RNA microhelices affect binding efficiency, but probably not the recognition process (two microhelices give similar footprints). Nucleotides in common between the two microhelices encompass the ones with an increased reactivity towards structural probes when in complex with tmRNA. Surprisingly, microhelix 1–3 is less stable in solution compared with microhelix 2, as shown by the absence of an RNase V_1-induced cleavage at position 19 (not shown).

Blocking the tmRNA ORF with antisense oligonucleotides does not impair its binding to either native or synthetic tRNA[Ala]

Antisense DNAs targeting the internal ORF of tmRNA might affect binding of either native or *in vitro* transcribed tRNA[Ala]. Antisense oligonucleotides with complementary regions including either one, two, three or all four alanine codons within the tmRNA internal ORF were designed (DNAs a–d, with DNA d blocking all 10 codons of the tmRNA ORF; Figure 9A), and their putative interference with tRNA[Ala] binding assayed. All four antisense oligonucleotides bind a complex between tmRNA and native tRNA[Ala1] or tRNA[Ala3], substantiated by RNase H-mediated cleavages of tmRNA when in complex with the antisense DNAs. In the presence of RNase H and each of the four antisense DNAs, a 5′-labeled tmRNA is entirely cleaved into an ~100-nucleotide fragment (Figure 9A). Since the mRNA module of *E.coli* tmRNA starts at position 90 and ends at position 122, this demonstrates that all four antisense DNAs bind within the tmRNA internal ORF. Notice that in the presence of DNA antisense c, two distinct RNase H-mediated cleavages are observed, whereas a single cut within the tmRNA ORF is induced by either DNA antisense a, b or d. This result probably reflects a dynamic equilibrium of binding of DNA c to tmRNA. DNA c, but not the other three DNAs, has to compete against an 11-base-pair stem (helix H4; Felden *et al.*, 1997) to bind the 3′ side of the tmRNA ORF. In the presence of each antisense DNA and compared with tRNA and tmRNA alone, the intensity of the gel-retarded band is not decreased (Figure 9B). Quantitation of the gel-retarded bands shows no difference with or without antisense DNAs. Similar results were obtained with synthetic tRNA[Ala2] (data not shown). These results suggest that the primary binding sites between tRNA[Ala] and tmRNA do not involve the tmRNA internal ORF. No detectable difference in the reactivity towards structural probes of the tRNA[Ala] anticodon loop with or without tmRNA (Figure 6) suggests that the tRNA[Ala] anticodon loop is also not involved.
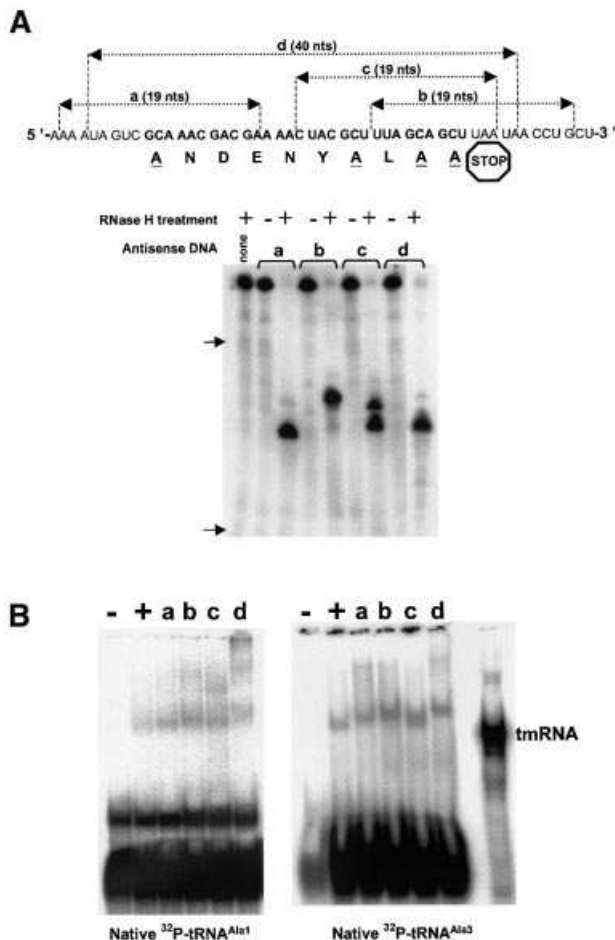
A

B

Fig. 9. (**A**) RNase H-mediated cleavages of the tmRNA internal ORF with four antisense DNA oligonucleotides. Five percent denaturing PAGE, with the upper arrow pointing to the Xylene cyanol dye (corresponds to the migration of an ~130mer) and the lower arrow pointing to the Bromophenol blue dye (corresponds to the migration of an ~30mer), respectively. a, b, c and d are the four antisense DNAs, and their respective targets within and around the tmRNA internal ORF are indicated. (**B**) Native gel retardation assays with antisense DNA oligonucleotides targeting the tmRNA internal ORF, in the presence of natives tRNA^Ala1 or tRNA^Ala3.

Active conformers of tmRNA are able to participate in complex formation with tRNA^Ala

After aminoacylation of tmRNA with [^3H]alanine by purified AlaRS and subsequent binding with tRNA^Ala3, 74 ± 26 d.p.m. of [^3H]alanine are in the complex lane between alanylated-tmRNA and tRNA^Ala, whereas there is no radioactivity in the complex lane between uncharged tmRNA and tRNA^Ala (Figure 10; three independent experiments). Consequently, complex formation between tmRNA and tRNA^Ala as a result of an artifact solely seen with inactive tmRNA conformers is excluded.

Discussion

General considerations

Native or synthetic tRNA^Ala isoacceptors from *E.coli* interact specifically with purified tmRNA from *E.coli in vitro*. tRNA^Ala post-transcriptional modifications
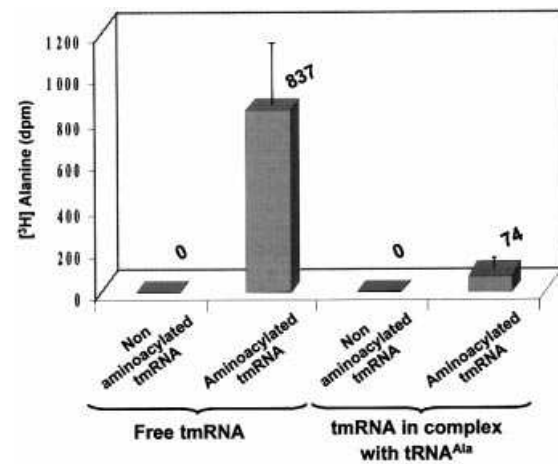

Fig. 10. Active conformers of tmRNA (aminoacylated form) are able to participate in complex formation with tRNA^Ala.

are important, but not essential, for binding tmRNA. Interestingly, native tRNA^Ala3 binds tmRNA much more tightly compared with native tRNA^Ala1, whereas their synthetic counterparts deprived of modified nucleosides bind tmRNA equally (Table I). Compared with native tRNA^Ala1, native tRNA^Ala3 has an additional post-transcriptional modification at position 34 (a uridine 5-oxyacetic acid) but lacks a modified uridine at position 8. Synthetic tRNA^Ala and tRNA^Ala microhelices bind tmRNA on a different basis compared with native tRNA^Ala. Engineering microhelices by chemical synthesis to introduce the two modified nucleosides at positions analogous to those present in the T-loops of canonical tRNAs might reveal their putative involvement in binding tmRNA. Binding plateaus between native-synthetic tRNA^Ala and tmRNA do not exceed several percent, with dissociation constants ranging from 0.5 (native tRNA^Ala3) to 3.5 μM (native tRNA^Ala1). Other native or synthetic tRNAs, such as tRNA^Asp or tRNA^Gln, do not bind tmRNA, suggesting that specific features within the tRNA^Ala structure allow the interaction to proceed. Four independent pieces of experimental evidence suggest that nucleotides within the acceptor stem of either native or synthetic tRNA^Ala are responsible for a specific interaction with tmRNA. First, using a variety of synthetic constructs derived from the sequence of tRNA^Ala, five nucleotides were identified, all in the acceptor stem, as being among those required to bind tmRNA. Secondly, structural probing of a synthetic tRNA^Ala indicates that when in the presence of tmRNA, nucleotides at positions 6 and 7 within the acceptor stem of tRNA^Ala become single stranded. Thirdly, structural probing of a native tRNA^Ala indicates that when in the presence of tmRNA, the first base pairs of the acceptor stem are significantly stabilized. Fourthly, RNA microhelices recapitulating a tRNA^Ala acceptor stem are able to bind tmRNA with specificity.

Kinetics of complex formation between tRNA^Ala and tmRNA

Plateau levels and dissociation constants (K_d) between tmRNA and various RNA constructs were measured and compared (Table I). As negative controls, *E.coli* or yeast tRNA^Asp, as well as *E.coli* tRNA^Gln, do not bind tmRNA.

Plateau levels and K_d between various tRNA^{Ala} constructs and tmRNA vary from 1 to 5% and from 0.5 to 3.5 µM, respectively. Full-length native and synthetic tRNA^{Ala} possess the higher binding plateaus, whereas one native tRNA^{Ala} isoacceptor and the RNA microhelices have higher dissociation constants (Table I). Direct comparison of both the binding plateaus and the K_d between synthetic tRNA^{Ala} 1, 2 and 3 and their corresponding RNA microhelices 1–3 and 2 is achievable. Compared with full-length tRNAs, the binding plateaus of the corresponding RNA microhelices are reduced 2-fold with a 2- to 4-fold decrease in their dissociation constants (Table I). These results suggest that compared with full-length tRNA^{Ala}, RNA microhelices bind tmRNA with more ease, accounting for a lower K_d, probably because they are three times smaller than full-length tRNAs. Their interaction with tmRNA, however, is probably not as stable as with full-length tRNA^{Ala}, as suggested by lower binding plateaus.

Structural basis of the interaction between tRNA^{Ala} and tmRNA

When tmRNA interacts with synthetic or native tRNA^{Ala}, only minor differences in the reactivity of nucleotides of both RNAs towards structural probes were detected. This could have been anticipated from only a few percent of complex formation out of total RNAs. Other subtle structural perturbations are probably not detected when the two RNAs interact with each other, with the approach described here, and await further structural mapping to be delineated. Footprints between tRNA^{Ala} and tmRNA were performed with native tRNA^{Ala3} and synthetic tRNA^{Ala2}, since gel retardation assays have shown that they bind tmRNA with the lower K_d (Table I). Within the tRNA^{Ala} structure, nucleotides with increased reactivity towards chemical and enzymatic probes are mostly clustered in the acceptor stem. For synthetic tRNA^{Ala2}, the acceptor stem partially unfolds when tmRNA binds. For RNA microhelices, the TψC loop unfolds. For native tRNA^{Ala3}, both the acceptor and the D stems are stabilized when tmRNA binds. Antisense oligonucleotides targeting the anticodon stem–loop of either native or synthetic tRNA^{Ala} increase its binding 2-fold (data not shown). This suggests a negative contribution of the anticodon stem–loop in complex formation, a result that is in agreement with a higher affinity of the RNA microhelices for tmRNA compared with their full-length tRNA counterparts. Specific interactions between tmRNA and either synthetic, native or minimalist tRNA^{Ala} structures are predicted to be different. Recognition between two RNAs might be very adaptable.

What are the sequences and/or structural domains within tmRNA involved in binding tRNA^{Ala} or the RNA^{Ala} microhelices? Within the ribose-phosphate backbone of tmRNA, specific cleavages appear when either tRNA^{Ala2}, tRNA^{Ala1-2} or RNA microhelix 2 interact with tmRNA (this is not observed with either native or synthetic tRNA^{Ala1} and tRNA^{Ala3}, or with microhelix 1–3). Thus, specific nucleotides from the acceptor stem of tRNA^{Ala2}, including G^5, C^6, C^{66}, G^{67} and C^{68}, trigger specific cuts within the tmRNA sequence. Interestingly, these tmRNA fragments still bind tRNA^{Ala} (or the microhelix) with specificity. Mapping these tmRNA fragments will identify the structural domains that are dispensable for binding synthetic tRNA^{Ala}. The band containing the tmRNA fragment in complex with synthetic tRNA^{Ala2} was excised from the gel, eluted passively and reverse transcribed with a DNA oligonucleotide complementary to the tmRNA 3′ end. A specific band with a length <280 nucleotides was obtained (data not shown). This demonstrates that these tmRNA fragments are missing at least the first 80 nucleotides from the 5′ end and are still capable of specific binding with tRNA^{Ala2}.

Biological significance of the interaction between tRNA^{Ala} and tmRNA

We report that native *E.coli* tmRNA interacts with two native tRNA^{Ala} isoacceptors from *E.coli* with affinity and specificity *in vitro*. Compared with tRNA^{Ala} isoacceptor 1, tRNA^{Ala} isoacceptor 3 binds tmRNA with a dissociation constant 7-fold lower and an ~2-fold higher binding plateau (Table I). Out of 46 tRNAs in *E.coli*, tRNA^{Ala} isoacceptor 3 is the seventh most abundant tRNA in *E.coli*. However, the intracellular concentration of each tRNA varies as a function of the growth rate. tmRNA is present in *E.coli* cells in low abundance, at ~500 copies per cell, at a growth rate for which ~5000 ribosomes are present (Lee *et al.*, 1978). Interestingly, at a similar condition of growth, native tRNA^{Ala} isoacceptor 3 represents 5% of the total tRNA population in *E.coli*, that is 3250 ± 220 molecules per cell (Ala3 is equivalent to Ala1B; Dong *et al.*, 1996). Thus, *in vivo*, there is a 6-fold excess of tRNA^{Ala3} compared with tmRNA. In these conditions, a complex can form *in vitro* between tRNA^{Ala3} and tmRNA. Native tRNA^{Ala} isoacceptor 1, however, represents only 0.95% of the total tRNA population in *E.coli* (620 ± 60 molecules per cell) and is one of the eight least abundant tRNAs in *E.coli* (Ala1 is equivalent to Ala2; Dong *et al.*, 1996).

Binding of native tmRNA to either native tRNA^{Ala1} or native tRNA^{Ala3} *in vitro* is stable at pHs varying between 5.0 and 8.0. All the *in vitro* binding assays were carried out at 37°C in the presence of monovalent (200 mM NH$_4$Cl), divalent (3 mM MgCl$_2$) and multivalent (10 mM spermidine) ions, at concentrations compatible with those in *E.coli* cells. Depending on the growth rate of *E.coli* cells, there is 5–6% of tRNA^{Ala3} (Dong *et al.*, 1996). Figure 2B demonstrates that tmRNA binds native tRNA^{Ala} isoacceptor 3 in the presence of all tRNAs from *E.coli*, even when there is only 5% of labeled tRNA^{Ala3} compared with total tRNAs. At a 200 molar excess of all tRNAs from *E.coli*, the binding between labeled tRNA^{Ala3} and tmRNA decreases slightly (~10%), which is likely to account for the competition of unlabeled tRNA^{Ala} isoacceptors from the mixture of all tRNAs with labeled tRNA^{Ala3} (Figure 2B). Moreover, active conformers of tmRNA (aminoacylated form) are able to participate in complex formation with tRNA^{Ala3} (Figure 10). However, this does not preclude an initial recognition between both uncharged tRNA^{Ala} and tmRNA, which are subsequently aminoacylated by a common aminoacyl-tRNA synthetase, AlaRS. Altogether, our results suggest that a specific complex between native tRNA^{Ala} isoacceptors and native tmRNA is likely to form *in vivo*. Considering the binding plateaus measured *in vitro*, and also that the stoichiometry between tRNA^{Ala} and tmRNA might be one-to-one *in vivo*, this

complex between tmRNA and tRNA^{Ala} could involve up to 140 tmRNA molecules out of the 500 per cell (1.5% of the 620 molecules of tRNA^{Ala1} and 4% of the 3250 molecules of tRNA^{Ala3}, in complex with tmRNA *in vitro*).

During *trans*-translation, the current model is that alanine-charged tmRNA recognizes stalled ribosomes, binds as a tRNA to the ribosomal A site, and donates the charged alanine to the nascent polypeptide chain via transpeptidation (for a review see Karzai *et al.*, 2000). The stalled mRNA is then replaced by tmRNA and resumption of translation ensues at an internal alanine (resume) codon in tmRNA. Out of 140 known tmRNA sequences from 118 species (tmRNA website; Williams, 2000), alanine is the resume codon for >80% of all tmRNA sequences, the remaining ones possessing either a glycine, an aspartic acid or a valine resume codon. This suggests that an alanine codon is preferred for resuming translation within the tmRNA internal ORF. For the other few species that use either glycine, aspartic acid or valine as resume codons in their respective tmRNA-mediated, protein-tagging systems, their tmRNA structures might allow specific recruitment of either tRNA^{Gly}, tRNA^{Asp} or tRNA^{Val}, but not tRNA^{Ala}. In *E.coli* tmRNA, mutating the resume codon from alanine (GCA) to either serine (UCA) or valine (GUA) still allows tagging of a truncated protein *in vivo* (Williams *et al.*, 1999), albeit to lower levels. However, tmRNA variants disallowing the proper utilization of the resume codon are not able to transfer the uncoded alanine attached to the 3′ end of tmRNA to the nascent polypeptide (Williams *et al.*, 1999). These data are in agreement with our results and suggest that tmRNA interacts with the tRNA that decodes the resume codon prior to entering the ribosome. *E.coli* tRNA^{Ala3} is the only isoacceptor with a 5′-UGC-3′ anticodon that can form three canonical pairs with the resume codon (5′-GCA-3′) from *E.coli* tmRNA. Here, we show that native tRNA^{Ala3} binds tmRNA with the highest affinity *in vitro* (Table I). Local recruitment and enrichment around tmRNA of the tRNA species that has to pair with the resume codon might help re-registration of the tag reading frame during *trans*-translation. Specific recruitment of tRNA^{Ala} by tmRNA involves structural domains outside of its internal ORF, but this does not exclude the possibility that the acceptor stem of tRNA^{Ala} has to be recognized first, with a subsequent recruitment of its anticodon loop at the resume codon. Defining the recognition elements within tmRNA that are required for binding tRNA^{Ala} with accuracy might reveal further biological insights.

Towards peptide bond formation between Ala-RNA^{Ala} and Ala-tmRNA^{Ala}

Alternatively, specific complex formation between tmRNA and tRNA^{Ala} might reflect only an ancient interaction between two aminoacylatable RNAs, when the translational apparatus might have required a covalent linkage between aminoacylated tRNAs and mRNAs, as for tmRNA, to recruit a second aminoacylated tRNA for peptide bond formation. If true, a small percentage of binding is only observed today, as putative remnants of these early events in the history of the genetic code. Aminoacylatable RNA microhelices were proposed to be present during these initial stages of the genetic code establishment (Tamura and Schimmel, 2001). Strikingly,

RNA microhelices also bind tmRNA, even with a 2- to 4-fold higher affinity compared with their full-length tRNA counterparts. Thus, our initial model for peptide bond formation will now be simplified further, a step forward towards defining the smallest machinery entirely made of RNAs capable of peptide bond formation, inspired from a molecule that is still functional in the 21st century.

Materials and methods

DNA oligonucleotides and enzymes

All the synthetic DNA oligonucleotides were synthesized by Cybergene (Saint-Malo, France). Four DNAs: 5′-TATTAAGCTGCTAAAGCG-TAGTTTTCGTCGTTTGCGACTA-3′, 5′-TTAAGCTGCTAAAGC-GTAG-3′, 5′-CAGGTTATTAAGCTGCTAA-3′ and 5′-TCGTCGTTT-GCGACTATTT-3′ were used as antisense targeting either tmRNA internal ORF. Thirteen DNA primers: 5′-GGGGATCCTGGTGGA-GGCGCGCGGG-3′, 5′-GTATGTTGTGTGGAATTGT-3′, 5′-GGA-AGCTTAATACGACTCACTATAGGGGGCATAGCTCAG-3′, 5′-GGG-GATCCTGGTGGAGCTATGCGG-3′, 5′-TAATACGACTCACTA-TA-3′, 5′-GGAAGCTTAATACGACTCACTATAGGGGCTATAGCT-CAG-3′, 5′-GGGGATCCTGGCGGAACGGACGGGAC-3′, 5′-TTA-AGTTGGGTAACGCCAG-3′, 5′-GGAAGCTTAATACGACTCACT-ATAGGAGCGGTAGTTCAG-3′, 5′-TGGTGGAGCTAGATCGAATAG-CCCCTATAGTGAGTCGTATTA-3′, 5′-TGGTGGAAGCGGATC-GAATGCCCCCTATAGTGAGTCGTATTA-3′, 5′-TGGTGGAGC-TGGCGGGA-3′ and 5′-TGGTGGAGCTGGC-3′ were used for cloning all of the synthetic tRNAs and for direct transcription of the RNA microhelices. T7 RNA polymerase was prepared according to Wyatt *et al.* (1991). Restriction enzymes *Bam*HI, *Hin*dIII, *Bst*N1, alkaline phosphatase and T4 polynucleotide kinase were from New England Biolabs (Beverly, MA). AMV reverse transcriptase, Taq DNA polymerase, T4 DNA ligase and T4 RNA ligase were from Gibco-BRL Life Technologies (Cergy-Pontoise, France). RNases S$_1$, V$_1$, U$_2$, and T$_1$ were from Amersham-Pharmacia-Biotech (Orsay, France). RNase H was from Sigma-Aldrich (Saint-Quentin, France). [γ-^{32}P]ATP (3000 mCi/mmol), [α-^{32}P]pCp (3000 mCi/mmol) and L-[3-^{3}H]alanine (74 Ci/mmol) were from NEN (Paris, France).

Preparation of RNAs and aminoacylation reaction

Escherichia coli tmRNA was overexpressed in *E.coli* cells and purified as previously described (Felden *et al.*, 1997). Synthetic RNAs were cloned downstream of a T7 RNA polymerase promoter as described (Perret *et al.*, 1990). Plasmids were linearized with *Bst*N1 restriction nuclease before transcription, so that *in vitro* transcribed RNAs will end with the 3′-terminal CCA triplet. *In vitro* transcription of synthetic tRNAs and RNA microhelices was performed as described (Felden *et al.*, 1994). Electrophoresis on denaturing gels separates the transcribed RNAs from non-incorporated nucleotides and DNA fragments. Appropriate bands were electroeluted, and pure *in vitro* transcribed RNAs were recovered by ethanol precipitation. Purified native tRNAs were from Subriden (Rolling Bay, WA). Aminoacylation reactions were performed in a medium containing 25 mM Tris–HCl pH 7.5, 7.5 mM MgCl$_2$, 2 mM ATP, 5 mM β-mercaptoethanol, 10 mM KCl, 200 pmol of tmRNA, 50 μM ^{3}H-labeled alanine and 700 nM purified *E.coli* AlaRS. Incubations were at 37°C for 30 min, then 200 mM cold potassium acetate pH 5.0 was added, followed by a phenol extraction of the enzyme at pH 4.3.

Gel retardation assays and structural mapping procedures

Labeling at the 5′ end of the RNAs was performed with [γ-^{32}P]ATP and phage T4 polynucleotide kinase after dephosphorylation with alkaline phosphatase (Silberklang *et al.*, 1977). Labeling at the 3′ end was carried out by ligation of [γ-^{32}P]pCp using T4 RNA ligase. After labeling, the RNAs were gel purified at a nucleotide resolution for tRNAs and RNA microhelices, eluted passively, and ethanol precipitated. RNAs were denatured for 2 min at 80°C in a folding buffer (5 mM MgCl$_2$, 20 mM NH$_4$Cl, 10 mM HEPES–KOH pH 6.9) and then slowly cooled down to room temperature for 30 min. Standard assays contained 0.5 pmol of labeled RNA in the presence of the appropriate concentration of aminoacylated or uncharged tmRNA in a binding buffer (10 mM spermidine, 3 mM MgCl$_2$, 200 mM NH$_4$Cl, 80 mM HEPES–KOH pH 6.9) to a final volume of 15 μl. A 30 min incubation at 37°C was either followed by enzymatic and chemical footprints between tRNA^{Ala} and

tmRNA, or subjected directly to electrophoresis in a 5% non-denaturing polyacrylamide gel, in 45 mM Tris–HCl pH 8.3, 43 mM boric acid, 0.1 mM MgCl$_2$ at 4°C and 10 V/cm (Ramos and Martínez-Salas, 1999). For the aminoacylated tmRNA, electrophoresis was in a 5% non-denaturing polyacrylamide gel overnight in 0.1 M Na acetate pH 5.0. Bands corresponding to aminoacylated tmRNA, either free or in complex with tRNA^{Ala3}, were excised, passively eluted in water, and ^{3}H was counted on a Wallac 1409 (Perkin-Elmer). Binding assays, gel excision, passive elution and counting were performed with uncharged tmRNA in identical conditions, as negative controls.

Digestions with the various ribonucleases (V$_1$ at 0.075 units, S$_1$ at 40 units, U$_2$ at 0.4 units and T$_1$ at 0.2 units) and probing with lead acetate (a final concentration of 2.5 mM) were performed as described (Felden *et al.*, 1997). Quantitation of selected bands was as described (Felden *et al.*, 1998). Relative amounts of RNA–RNA complexes were analyzed on a PhosphorImager with ImageQuant (Molecular Dynamics, Sunnyvale, CA). Data are represented as the percentage of the RNA complex of interest relative to the input probe, calculated as the sum of the intensity of all bands in the corresponding lane.

Inhibition assays with antisense DNA oligonucleotides
Four synthetic DNA oligonucleotides complementary to various portions of the tmRNA ORF were used. For annealing, 100 pmol of tmRNA or tRNA and 1000 pmol of an oligonucleotide were incubated in folding buffer for 2 min at 80°C. After annealing, gel retardation assays were performed as described. RNase H digestion assays of antisense DNA–tmRNA duplexes were adapted from Matveeva *et al.* (1997); both the molar ratio between the antisense DNAs and tmRNA as well as the annealing step were as for the binding assays between tmRNA, labeled tRNAs and the antisense DNAs shown in Figure 9B.

Acknowledgements

References

Abo,T., Inada,T., Ogawa,K. and Aiba,H. (2000) SsrA-mediated tagging and proteolysis of LacI and its role in the regulation of lac operon. *EMBO J.*, **19**, 3762–3769.

Dong,H., Nilsson,L. and Kurland,C.G. (1996) Co-variation of tRNA abundance and codon usage in *Escherichia coli* at different growth rates. *J. Mol. Biol.*, **260**, 649–663.

Felden,B., Florentz,C., Giegé,R. and Westhof,E. (1994) Solution structure of the 3′-end of brome mosaic virus genomic RNAs. Conformational mimicry with canonical tRNAs. *J. Mol. Biol.*, **235**, 508–531.

Felden,B., Himeno,H., Muto,A., McCutcheon,J.P., Atkins,J.F. and Gesteland,R.F. (1997) Probing the structure of the *Escherichia coli* 10Sa RNA (tmRNA). *RNA*, **3**, 89–103.

Felden,B., Hanawa,K., Atkins,J.F., Himeno,H., Muto,A., Gesteland,R.F., McCloskey,J.A. and Crain,P.F. (1998) Presence and location of modified nucleotides in *Escherichia coli* tmRNA: structural mimicry with tRNA acceptor branches. *EMBO J.*, **17**, 3188–3196.

Francklyn,C. and Schimmel,P. (1989) Aminoacylation of RNA minihelices with alanine. *Nature*, **337**, 478–481.

Huang,C., Wolfgang,M.C., Withey,J., Koomey,M. and Friedman,D.I. (2000) Charged tmRNA but not tmRNA-mediated proteolysis is essential for *Neisseria gonorrhoeae* viability. *EMBO J.*, **19**, 1098–1107.

Hutchison,C.A., Peterson,S.N., Gill,S.R., Cline,R.T., White,O., Fraser,C.M., Smith,H.O. and Venter,J.C. (1999) Global transposon mutagenesis and a minimal Mycoplasma genome. *Science*, **286**, 2165–2169.

Karzai,A.W., Roche,E.D. and Sauer,R.T. (2000) The SsrA-SmpB system for protein tagging, directed degradation and ribosome rescue. *Nature Struct. Biol.*, **7**, 449–455.

Kholod,N.S. (1999) Dimer formation by tRNAs. *Biochemistry (Mosc.)*, **64**, 298–306.

Komine,Y., Kitabatake,M., Yokogawa,T., Nishikawa,K. and Inokuchi,H. (1994) A tRNA-like structure is present in 10Sa RNA, a small stable RNA from *Escherichia coli*. *Proc. Natl Acad. Sci. USA*, **91**, 9223–9227.

Lee,N., Bessho,W., Weil,K., Szostak,J.W. and Suga,H. (2000) Ribozyme-catalyzed tRNA aminoacylation *Nature Struct. Biol.*, **7**, 28–33.

Lee,S.Y., Bailey,S.C. and Apirion,D. (1978) Small stable RNAs from *Escherichia coli*: evidence for the existence of new molecules and for a new ribonucleoprotein particle containing 6S RNA. *J. Bacteriol.*, **133**, 1015–1023.

Matveeva,O., Felden,B., Audlin,S., Gesteland,R.F. and Atkins,J.F. (1997) A rapid *in vitro* method for obtaining RNA accessibility patterns for complementary DNA probes: correlation with an intracellular pattern and known RNA structures. *Nucleic Acids Res.*, **25**, 5010–5016.

Muth,G.W., Ortoleva-Donnelly,L. and Strobel,S.A. (2000) A single adenosine with a neutral pK_a in the ribosomal peptidyl transferase center. *Science*, **289**, 947–950.

Muto,A., Fujihara,A., Ito,K.I., Matsuno,J., Ushida,C. and Himeno,H. (2000) Requirement of transfer-messenger RNA for the growth of *Bacillus subtilis* under stresses. *Genes Cells*, **5**, 627–635.

Nissen,P., Hansen,J., Ban,N., Moore,P.B. and Steitz,T.A. (2000) The structural basis of ribosome activity in peptide bond synthesis. *Science*, **289**, 920–930.

Noller,H.F., Hoffarth,V. and Zimniak,L. (1992) Unusual resistance of peptidyl transferase to protein extraction procedures. *Science*, **256**, 1416–1419.

Perret,V., Garcia,A., Puglisi,J., Grosjean,H., Ebel,J.-P., Florentz,C. and Giegé,R. (1990) Conformation in solution of yeast tRNA^{Asp} transcripts deprived of modified nucleotides. *Biochimie*, **72**, 735–743.

Piccirilli,J.A., McConnell,T.S., Zaug,A.J., Noller,H.F. and Cech,T.R. (1992) Aminoacyl esterase activity of the *Tetrahymena* ribozyme. *Science*, **256**, 1420–1424.

Ramos,R. and Martínez-Salas,E. (1999) Long-range RNA interactions between structural domains of the aphthovirus internal ribosome entry site (IRES). *RNA*, **5**, 1374–1383.

Schimmel,P., Giegé,R., Moras,D. and Yokoyama,S. (1993) An operational RNA code for amino acids and possible relationship to genetic code. *Proc. Natl Acad. Sci. USA*, **90**, 8763–8768.

Silberklang,M., Prochiantz,A., Haenni,A.L. and Rajbhandary,U.L. (1977) Studies on the sequence of the 3′-terminal region of turnip-yellow-mosaic-virus RNA. *Eur. J. Biochem.*, **72**, 465–478.

Sprinzl,M., Horn,C., Brown,M., Ioudovitch,A. and Steinberg,S. (1998) Compilation of tRNA sequences and sequences of tRNA genes. *Nucleic Acids Res.*, **26**, 148–153.

Tamura,K. and Schimmel,P. (2001) Oligonucleotide-directed peptide synthesis in a ribosome- and ribozyme-free system. *Proc. Natl Acad. Sci. USA*, **98**, 1393–1397.

Ushida,C., Himeno,H., Watanabe,T. and Muto A. (1994) tRNA-like structures in 10Sa RNAs of *Mycoplasma capricolum* and *Bacillus subtilis*. *Nucleic Acids Res.*, **22**, 3392–3396.

Varani,V. and McClain,W.H. (2000) The G·U wobble base pair: a fundamental building block of RNA structure crucial to RNA function in diverse biological systems. *EMBO rep.*, **1**, 18–23.

Williams,K.P. (2000) The tmRNA website. *Nucleic Acids Res.*, **28**, 168.

Williams,K.P., Martindale,K.A. and Bartel,D.P. (1999) Resuming translation on tmRNA: a unique mode of determining a reading frame. *EMBO J.*, **18**, 5423–5433.

Williams,R.J., Nagel,W., Roe,B. and Dudock,B. (1974) Primary structure of *E.coli* alanine transfer RNA: relation to the yeast phenylalanyl tRNA synthetase recognition site. *Biochem. Biophys. Res. Commun.*, **60**, 1215–1221.

Wyatt,J.R., Chastain,M. and Puglisi,J.D. (1991) Synthesis and purification of large amounts of RNA oligonucleotides. *Biotechniques*, **11**, 764–769.

Zhang,B. and Cech,T.R. (1997) Peptide bond formation by *in vitro* selected ribozymes. *Nature*, **390**, 96–100.